MOLECULAR AND CELLULAR BIOLOGY, Sept. 2006, p. 6844–6858 Vol. 26, No. 18
0270-7306/06/$08.00+0 doi:10.1128/MCB.00283-06

The Rho-mDia1 Pathway Regulates Cell Polarity and Focal Adhesion Turnover in Migrating Cells through Mobilizing Apc and c-Src†

Norikazu Yamana,[1,2]‡ Yoshiki Arakawa,[1,2]‡# Tomohiro Nishino,[1] Kazuo Kurokawa,[3]‖ Masahiro Tanji,[1,2] Reina E. Itoh,[3] James Monypenny,[1] Toshimasa Ishizaki,[1] Haruhiko Bito,[1]§ Kazuhiko Nozaki,[2] Nobuo Hashimoto,[2] Michiyuki Matsuda,[3]¶ and Shuh Narumiya[1]*

Department of Pharmacology[1] and Department of Neurosurgery,[2] Kyoto University Faculty of Medicine, Kyoto 606-8501, Japan, and Department of Signal Transduction, Research Institute for Microbial Diseases, Osaka University, Osaka 565-0871, Japan[3]

Received 15 February 2006/Returned for modification 13 March 2006/Accepted 29 June 2006

Directed cell migration requires cell polarization and adhesion turnover, in which the actin cytoskeleton and microtubules work critically. The Rho GTPases induce specific types of actin cytoskeleton and regulate microtubule dynamics. In migrating cells, Cdc42 regulates cell polarity and Rac works in membrane protrusion. However, the role of Rho in migration is little known. Rho acts on two major effectors, ROCK and mDia1, among which mDia1 produces straight actin filaments and aligns microtubules. Here we depleted mDia1 by RNA interference and found that mDia1 depletion impaired directed migration of rat C6 glioma cells by inhibiting both cell polarization and adhesion turnover. Apc and active Cdc42, which work together for cell polarization, localized in the front of migrating cells, while active c-Src, which regulates adhesion turnover, localized in focal adhesions. mDia1 depletion impaired localization of these molecules at their respective sites. Conversely, expression of active mDia1 facilitated microtubule-dependent accumulation of Apc and active Cdc42 in the polar ends of the cells and actin-dependent recruitment of c-Src in adhesions. Thus, the Rho-mDia1 pathway regulates polarization and adhesion turnover by aligning microtubules and actin filaments and delivering Apc/Cdc42 and c-Src to their respective sites of action.

Cell migration is indispensable in biological processes such as development, inflammation, wound healing, and tumor metastasis. Migrating cells polarize by extending protrusions at the front and retracting the tail at the rear, and make adhesions to extracellular matrix (ECM) to stabilize the forward protrusion (36). Adhesions to ECM are then used as sites to pull the cell body forward and are subsequently disassembled as the cell moves over them. This cycle of events enables cells to migrate to their destination. The actin cytoskeleton and microtubules (MTs) work critically in these events. Actin polymerization at the leading edge drives membrane protrusion, the association of the actin cytoskeleton with integrins regulates binding of the integrins to ECM, and the actin bundles within the body generate tension to pull the cell body forward and retract the tail. MTs are also polarized in migrating cells and are essential for the directed migration of many cell types (36, 37). However, how these cytoskeletons are regulated in migrating cells and work for cell polarization and adhesion turnover remains largely unknown.

The Rho GTPases, including Rho, Rac, and Cdc42, work as molecular switches in cell morphogenesis by inducing specific types of actin cytoskeleton and by locally regulating MT dynamics. Accumulating evidence suggests that Cdc42 regulates cell polarity and Rac works in membrane protrusion of migrating cells. Indeed, Cdc42 is active at the cell front (17, 30), and disruption of Cdc42 function impairs directionality of migration in many cell types (1, 32). One well-characterized action of Cdc42 in cell polarity is to orient the MT organizing center (MTOC) in the front of the nucleus toward the leading edge (8, 32), though the significance of this action in directed migration remains to be established. Rac is also active in the front of migrating cells (17, 20) and is thought to induce membrane protrusion by stimulating actin polymerization through activation of the WAVE-Arp2/3 complex pathway (5). In contrast to these findings on Cdc42 and Rac, the role of Rho in cell migration has been difficult to assess. Roles of Rho in physiological processes can be analyzed by the use of botulinum C3 exoenzyme (40). However, treatment with C3 exoenzyme elicits different effects on cell morphogenesis and migration that are dependent on the dose of the enzyme (2, 32, 42), and complete inactivation of Rho abolishes cell adhesion (32) and chemotactic response (1) almost completely, making interpretation and further analysis difficult. Two major effectors, Rho-associated kinase (ROCK) and mammalian homologue of the *Drosophila* gene *Diaphanous 1* (mDia1), mediate Rho actions: ROCK by inducing actomyosin contraction and inhibiting actin filament disassembly (19, 24) and mDia1 by catalyzing actin polymerization and regulating MT dynamics (14, 16, 23, 45). Roles of ROCK have been analyzed by the use of a specific

* Corresponding author. Mailing address: Department of Pharmacology, Kyoto University Faculty of Medicine, Kyoto 606-8501, Japan. Phone: 81-75-753-4392. Fax: 81-75-753-4693. E-mail: snaru@mfour.med.kyoto-u.ac.jp.

† Supplemental material for this article may be found at http://mcb.asm.org/.

‡ N.Y. and Y.A. contributed equally to this work.

Present address: Cell Motility Laboratory, Cancer Research UK, London WC2A 3PX, United Kingdom.

‖ Present address: Molecular Membrane Biology Laboratory, RIKEN Discovery Research Institute, Saitama 351-0198, Japan.

§ Present address: Department of Neurochemistry, University of Tokyo Graduate School of Medicine, Tokyo 113-0033, Japan.

¶ Present address: Department of Pathology and Biology of Diseases, Kyoto University Faculty of Medicine, Kyoto 606-8501, Japan.

inhibitor, Y-27632 (43), and one of these studies revealed the involvement of ROCK in tail retraction (50). On the other hand, until recently there has been no specific tool available to analyze the role of mDia1. We recently developed an RNA interference (RNAi) technique for mDia1 and characterized the role of mDia1 in axon elongation (2). Applying this strategy, we have now examined the role of the Rho-mDia1 pathway in cell polarity and migration.

MATERIALS AND METHODS

Materials. Short interfering double-stranded RNA oligomers (siRNAs) K2 and A6, targeting the nucleotide sequences from positions 795 to 813 (2) and 184 to 209 (GCGACGGCGGCAAACATAAGAAATT), respectively, of mDia1 (NM_007858) were used for RNAi for mDia1. pEGFP constructs for mDia1 and mutants, pFL-mDia1-ΔN3, pEGFP-Histone H2B, and glutathione *S*-transferase (GST)–PAK CRIB were described previously (2, 16, 33, 42, 46). pRaichu-Rac and pRaichu-Cdc42, which consist of cyan fluorescent protein (CFP) and yellow fluorescent protein (YFP), were described previously (17). SDF-1α was purchased from PeproTech EC. PP1 was purchased from BIOMOL. SU6656 and latrunculin B were from Calbiochem, and nocodazole was from Sigma-Aldrich. pEGFP-C1 was from CLONTECH. pCAG-myc-c-Src will be described elsewhere. Yellow fluorescent protein (YFP)-paxillin was a gift from C. Ballestrem and A. D. Bershadsky, The Weizmann Institute of Science, Rehovot, Israel. Anti-Apc antibody was a gift of Inke Näthke, University of Dundee, Dundee, United Kingdom. Rabbit polyclonal antibody to mDia2 will be described elsewhere. Other primary antibodies used are polyclonal antibody to pericentrin (Covance); polyclonal antibody to p130Cas (29); monoclonal antibodies to β-actin and β-tubulin (Sigma-Aldrich); antibody to p140mDia (BD Bioscience); antibodies to Cdc42 (B-8), mDia3 (N15), and c-Myc (A-14) (Santa Cruz Biotechnology); monoclonal antibodies to phosphotyrosine (4G10), Src (GD11), and Rac1 (Upstate Biotechnology); antibody to green fluorescent protein (GFP; Molecular Probes); antibodies to Glu tubulin, α-tubulin, and vinculin (Chemicon); antibody to Src (pY418) (Biosource International); and antibody to p130Cas (Tyr410) (Cell Signaling Technology). Alexa Fluor 488-, 594-, 633-conjugated goat antibodies to rabbit, rat, and mouse immunoglobulin G and Alexa Fluor 594- and 633-phalloidin were purchased from Molecular Probes.

Transfection and migration assays. Rat C6 glioma cells, NIH 3T3 cells, and HeLa cells were cultured in Dulbecco's modified Eagle's medium (DMEM) with 10% fetal bovine serum (FBS). HEK 293 cells were cultured in DMEM/Ham's F-12 with 10% FBS. Transfection was performed as described previously (2). In migration assays, C6 glioma cells were transfected with (EGFP) alone or together with either control or mDia1 siRNA and used 24 h later. SDF-1α exerted a bell-shaped chemotactic response in these cells, with a peak effect at 100 to 250 ng/ml (data not shown). In the transwell assay, transwell invasion chambers (BD BioCoat Matrigel) were used. Transfected C6 cells (1.0×10^5 cells per well) were added to the upper compartment, and SDF-1α was added to the lower compartment at 250 ng/ml. The number of cells that migrated across the membrane was determined 24 h later. In the wound-healing assay, cells grown to 70% confluence were transfected. The monolayer was scratched with a sterile pipette tip 24 h later. For MTOC orientation, MTOC was stained with an antipericentrin antibody and scored as positive orientation when MTOC localized within a 90° sector facing directly toward the wound edge. In the assay using the direct-viewing Dunn chemotaxis chamber (Weber Scientific International, United Kingdom) (1, 53), the chambers were placed under an epifluorescence microscope (model IX81; Olympus) equipped with a charge-coupled device (CCD) camera (MMX-512BFT; Roper Scientific) controlled by MetaMorph software (Universal Imaging Corp.). C6 glioma cells were plated on a coverglass and transfected. The coverglass was then assembled onto the chamber, and 100 ng/ml SDF-1α was then applied in the outer well. A field of cells positioned directly above the diffusion gap was then selected for time-lapse observation for 6 h. One image was acquired every 15 min, and the video sequences were subsequently constructed from these sequential images.

C3 exoenzyme treatment. Botulinum C3 exoenzyme was prepared as described previously (28) and added at 30 μg/ml to a C6 cell monolayer 12 h before making a wound. The wound-healing assay was carried out in the continued presence of C3 exoenzyme for 8 h. Because insufficient treatment with C3 exoenzyme can lead to preferential suppression of the ROCK pathway and keep the mDia1 pathway intact (2, 39), we extensively treated C6 glioma cells with C3 exoenzyme and subjected to the analysis only experiments in which the treated cells showed the "C3 phenotype": that is, a round cell body with beaded processes containing bundled MTs (15).

Microscopy and image acquisition. Fluorescence staining was performed essentially as described previously (2, 42). For Cdc42 and Apc staining, cells were fixed 8 h after the wounding with 3.7% paraformaldehyde in phosphate-buffered saline (PBS) and extracted for 30 s with 0.5% Triton X-100 in PHEM buffer, composed of 60 mM PIPES [piperazine-*N*,*N*′-bis(2-ethanesulfonic acid)], 25 mM HEPES, 10 mM EGTA, and 1 mM Mg acetate (pH 6.9). Images were acquired using an oil immersion objective (×60, 1.4 NA) and an Olympus BX52 microscope equipped with a Roper CoolSnap-HQ CCD camera. The system was steered by MetaMorph, and each signal was given a pseudocolor in merged images. Where indicated, cells were fixed with methanol at −20°C for 10 min, permeabilized with 0.1% Triton X-100 in PBS for 5 min, and stained for Apc. Confocal images were acquired using a Zeiss LSM510 Meta system with a ×63 PlanAPO(1.4) oil immersion objective. Fluorescent resonance energy transfer (FRET) imaging was performed essentially as described previously (17, 27) using cells cotransfected with siRNAs and pRaichu-Rac or pRaichu-Cdc42. After 24 h, the wound was made, and images were acquired using a microscope (model IX70; Olympus) equipped with a Roper CoolSnap-HQ CCD camera and controlled by MetaMorph. For focal adhesion imaging, cells were cotransfected with either control or mDia1 siRNA and YFP-paxillin. The cells were subjected to a wound-healing assay, and YFP fluorescence was monitored for 4 h. To examine adhesion turnover, the initial position of each adhesion within the first frame of the movie was marked and its turnover was monitored over subsequent frames.

Immunochemical analysis. Immunoprecipitation and Western blot analysis were performed as described previously (2, 42). For the immunoprecipitation shown in Fig. 8A, we used the following buffer: 20 mM Tris-HCl, pH 7.5, 100 mM NaCl, 2 mM dithiothreitol, 1 mM sodium fluoride, 1 mM sodium orthovanadate, 0.1% Triton X-100, and a protease inhibitor mixture. For preparation of the membrane fraction, the cells were lysed in a hypotonic buffer (10 mM HEPES-NaOH, pH 7.5) containing 10 mM KCl, 2 mM $MgCl_2$, and a protease inhibitor mixture. After nuclei were removed by centrifugation at $600 \times g$ for 10 min, the membrane fraction was collected by centrifugation at $100{,}000 \times g$ for 60 min. The pull-down assay for GTP-Rac was performed as described previously (42).

Statistical analysis. Data are presented as mean ± standard error of the mean and were analyzed by Student's *t* test with Prism 4.0 software. A P value of <0.05 was considered statistically significant.

RESULTS

The Rho-mDia1 pathway is required for rat glioma cell migration. Rat C6 glioma cells were used and subjected to RNAi for mDia1. We used two siRNAs, K2 and A6, targeting different nucleotide sequences of mDia1. Western blot analysis revealed that transfection of these cells with K2 but not with control scrambled siRNA reduced the amount of endogenous mDia1 by approximately 50%, while K2 did not reduce the amount of other mDia isoforms, mDia2 and mDia3 (Fig. 1A). Transfection with mDia1 siRNA A6 also potently and selectively reduced the amount of mDia1. We then cotransfected the cells with EGFP and each of these mDia1 siRNAs and examined depletion of mDia1 in individual transfected cells. EGFP was expressed in around 25% of cells in each experiment, more than 90% of which showed little signal for mDia1, suggesting that mDia1 was depleted with either siRNA almost completely in EGFP-expressing cells (Fig. 1B; data not shown). We therefore used EGFP as a marker for RNAi and examined effects of depletion of mDia1 on cell morphology and functions. We first used siRNA K2 and examined its effects. mDia1-RNAi with K2 neither changed morphology and cytoskeletal organization of C6 glioma cells under the basal conditions nor affected cytokinesis (see Fig. S1 in the supplemental material). However, mDia1-RNAi with K2 specifically suppressed migration of glioma cells to stroma cell-derived factor 1α (SDF-1α) in a transwell assay (Fig. 1C). Suppression of migration was also seen in C6 glioma cells expressing a

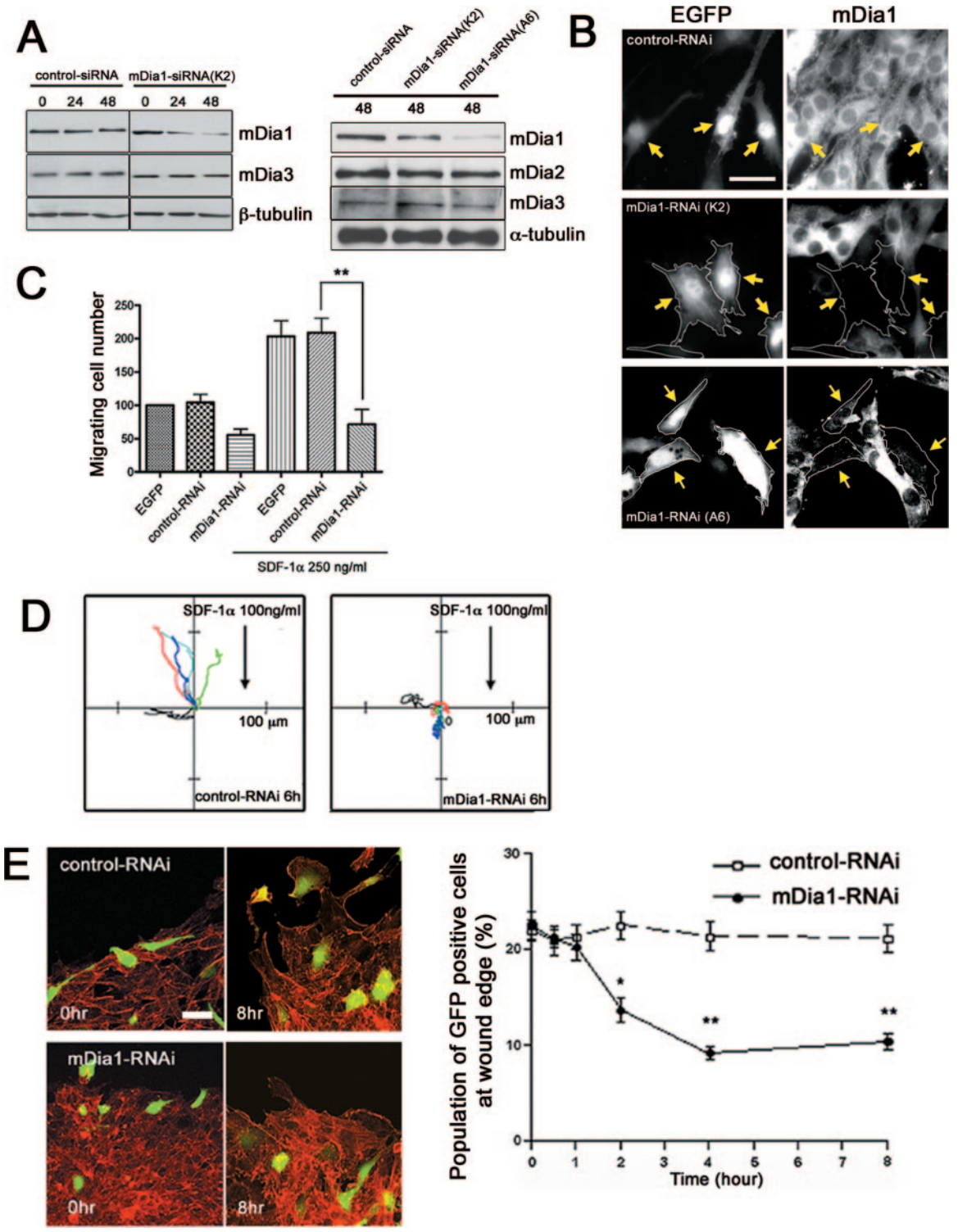

FIG. 1. mDia1 regulates directed migration of rat C6 glioma cells. (A and B) RNAi for mDia1. C6 glioma cells were transfected with siRNA for mDia1 (either K2 or A6 or control scrambled siRNA) and were collected at 0, 24, and 48 h. Depletion of mDia1 was examined by Western blot analysis (A) and by immunofluorescence (B). (C) Cell migration in a Matrigel transwell assay. C6 glioma cells were transfected with EGFP alone or together with either control scrambled siRNA or mDia1 siRNA K2 and subjected to the assay as described in Materials and Methods. (D) Cell migration in a Dunn chamber. Migration was recorded by time-lapse video for 6 h. Panels show the trajectories of individual cells generated by interactive tracking of the film data and coded in different colors ($n = 5$ each). (E) Cell migration in an in vitro wound-healing assay. Cells cotransfected with EGFP and either control scrambled siRNA or mDia1 siRNA K2 were subjected to a wound-healing assay. Typical images at 0 and 8 h are shown (left). The number of EGFP-expressing cells at the wound edge was determined at the indicated times (right). * and **, $P < 0.05$ and $P < 0.01$, respectively, versus control RNAi cells. Scale bars, 20 μm. Typical results of more than five independent experiments are shown for each analysis.

putative dominant-negative mDia1 mutant (42) or cells treated with C3 exoenzyme but not with Y-27632 (see Fig. S2 in the supplemental material). These results show that the Rho-mDia1 pathway works critically in directed migration of the glioma cells.

We next examined chemotaxis of these cells in the Dunn chamber (1, 53). Control RNAi cells migrated toward SDF-1α with the elongated morphology, whereas the K2-mediated mDia1-RNAi cells exhibited a spread morphology and poor motility (see videos S1 and S2 in the supplemental material). Trajectory analysis revealed that both directionality and locomotion were suppressed in mDia1-depleted cells (Fig. 1D). We also examined migration of K2-mediated mDia1-RNAi cells in an in vitro wound-healing assay (Fig. 1E). We found that approximately 20 to 25% of the wound-edge cell population consisted of EGFP-expressing cells at the beginning of each experiment. This number remained the same over the 8-h observation period for control RNAi cells. In contrast, the EGFP-expressing mDia1-RNAi cells were left behind during the process of wound closure and the percentage of EGFP-expressing cells decreased to <10%.

The Rho-mDia1 pathway is required for cell polarization and focal adhesion turnover. Because the above results suggest that mDia1 is implicated in both polarization and locomotion of migrating cells, we examined the effects of mDia1 depletion on each aspect. We first examined cell polarity using three parameters, MT polarity, MTOC orientation, and localization of active Rac. Gundersen and colleagues (4, 49) reported that a subset of MTs is stabilized toward the direction of cell migration and becomes detyrosinated in a Rho-dependent manner, and they suggested that mDia mediates this MT stabilization. Consistent with their suggestion, we found that MTs containing detyrosinated Glu tubulin were present in control cells, but almost absent in mDia1-RNAi cells (see Fig. S3 in the supplemental material). We next examined MTOC orientation (8). When the cells at the edge of the wound were examined during the course of wound closure, the percentage of cells showing a positive MTOC orientation increased from 25% to over 60% in control RNAi cells, whereas the value in K2-mediated mDia1 RNAi cells that remained at the wound edge was suppressed to approximately 30% (Fig. 2A). This effect of mDia1 depletion is again consistent with the results of experiments using C3 exoenzyme and Y-27632 (Fig. 2B), suggesting the role of the Rho-mDia1 pathway in cell polarization. Finally, we examined localization of active Rac in mDia1-RNAi cells. Recent FRET analysis revealed that GTP-bound active Rac accumulates in the leading lamella and gradually decreases toward the tail (17, 20). Using Raichu-Rac as a probe (17), we identified a similar distribution of active Rac in control RNAi cells subjected to the wound-healing assay, whereas no such gradient was found in K2-mdiated mDia1-RNAi cells where active Rac appeared to be distributed evenly throughout the cell (Fig. 2C). Video microscopy revealed that membrane ruffling occurs mostly in the leading edge in control RNAi cells, whereas weak ruffles were seen all around cell periphery in the mDia1-RNAi cells (see videos S3 and S4 in the supplemental material). These results demonstrated that mDia1 functions critically in cell polarization. We next addressed how depletion of mDia1 suppresses cell locomotion by analyzing adhesion turnover. We expressed YFP-paxillin as a marker for focal adhesions and examined their dynamics by video microscopy (22, 52). YFP-paxillin exhibited numerous wedge-like signals of focal adhesions in control RNAi cells, and they turned over quickly as the cell moved to the wound during the 3-h observation period (Fig. 3). In contrast, focal adhesions turned over poorly in a K2-mediated mDia1-RNAi cell, and the cell did not migrate appreciably (see videos S5 and S6 in the supplemental material). Quantitative analysis of three cells of each group revealed that 184 out of 242 adhesions turned over within 1 h in control RNAi cells, whereas only 69 out of 255 turned over within this period in the mDia1 RNAi cells (Fig. 3). Thus, the numbers of adhesions were not different between the two groups, indicating that adhesions are formed normally in mDia1 RNAi cells. Consistently, mDia1-RNAi cells formed focal adhesions over a time course similar to that of control cells during spreading, although turnover of these adhesions was impaired, resulting in delayed cell spreading (unpublished observation).

Thus far, we used siRNA K2 and analyzed the effects of mDia1 depletion on cell migration. However, given that any siRNA can sometimes exert nonselective effects, we examined effects of transfection with a different siRNA A6 on cell migration and polarity. Transfection with this siRNA again interfered with migration, MTOC orientation, and focal adhesion turnover of C6 glioma cells subjected to the wound-healing assay (see Fig. S4 in the supplemental material).

mDia1 mediates localization of Cdc42 and Apc in the front of migrating cells. To obtain an insight into how mDia1 regulates cell polarization, we next examined the effects of mDia1 depletion on localization of Cdc42 and Apc in the leading edge of migrating cells. Apc and Cdc42 have been shown to be present in this region and function for cell polarization (8, 9). Immunofluorescence for Cdc42 revealed that most of the Cdc42 signals accumulated in the perinuclear region, but a significant population of the signals were seen as dot-like structures in the leading edge of control migrating cells (Fig. 4A). Notably most of these dots in the periphery were seen on MTs. These dot-like Cdc42 signals were significantly reduced, and little association with MTs was found in mDia1-RNAi cells. Since the immunofluorescence signal represents the total population of Cdc42, we next performed FRET analysis using Raichu-Cdc42 (17) and examined localization of active Cdc42. This analysis revealed prominent Cdc42 activity in the leading edge of migrating cells, while no such signals were seen in the mDia1 RNAi cells (Fig. 4B; see also videos S7 and S8). When three different cells each from control and mDia1 RNAi groups were examined, all three of the control RNAi cells showed a gradient of Cdc42 activity from the front to the tail, but none of the mDia1 RNAi cells exhibited such a gradient (Fig. 4B). These results indicate that mDia1 is responsible for accumulation or maintenance of active Cdc42 at the leading edge. We next performed immunofluorescence for Apc. Signals for Apc were mostly concentrated in the perinuclear region, but, as reported previously (26, 31), a part of the Apc signal was found in dot-like structures at the plus ends of MTs in the tip of control migrating cells. However, these signals were scarcely seen in mDia1-RNAi cells (Fig. 4C). Our findings on Apc and Cdc42 were not due to down-regulation of Apc and Cdc42 in mDia1-depleted cells, because the Western blot analysis showed no difference in expression of Apc or

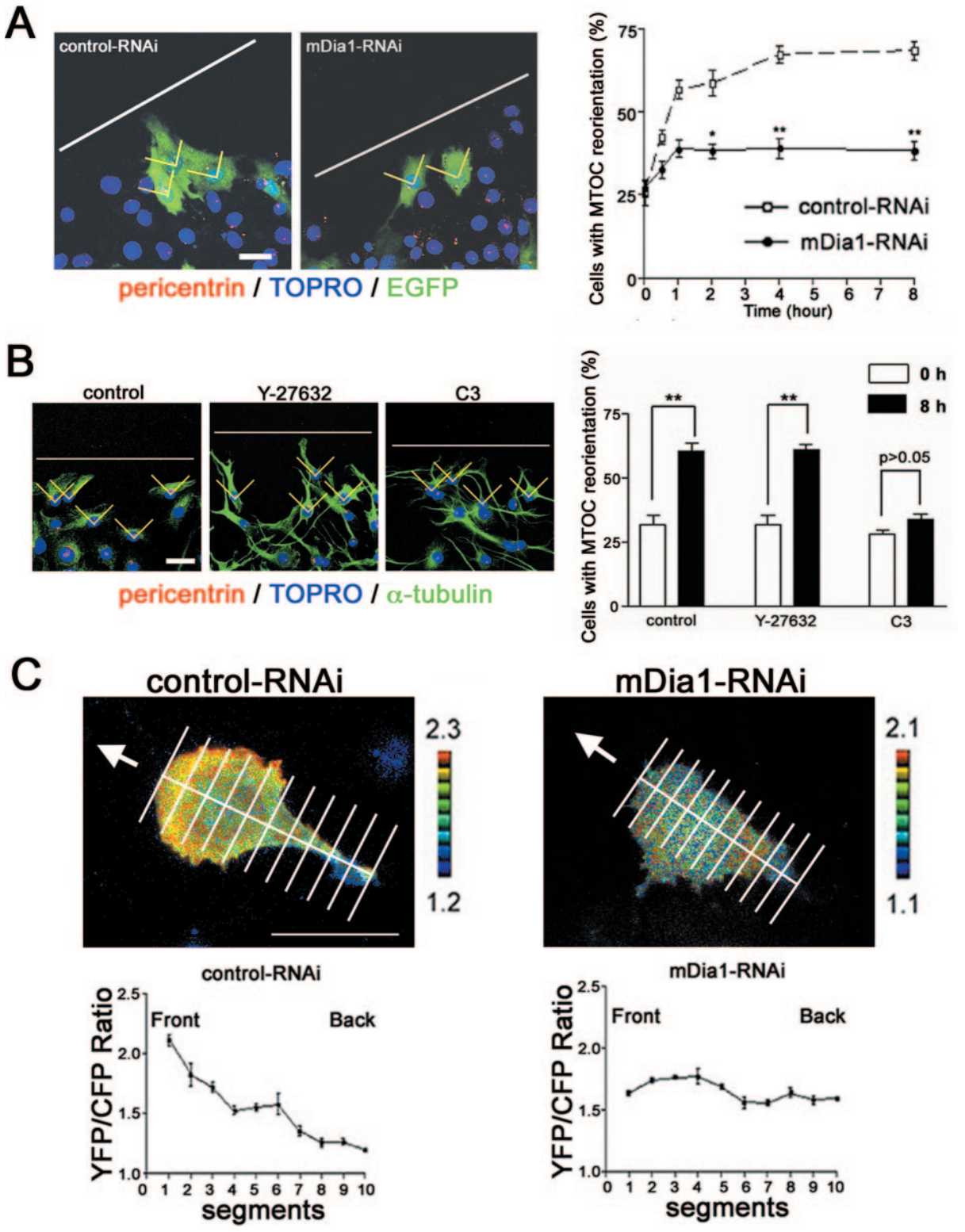

FIG. 2. Rho-mDia1 pathway is required for polarization of migrating cells. (A) Impaired MTOC orientation in mDia1-depleted cells. The percentage of control and K2-mediated mDia1 RNAi cells showing MTOC oriented toward the wound (borders and wound edge shown in yellow and white, respectively) is shown ($n = 50$ for each of three independent experiments for each group for each time point). * and **, $P < 0.05$ and $P < 0.01$, respectively, versus control cells. We scored MTOC orientation as positive when MTOC localized within a 90° sector (borders are shown in yellow) facing directly toward the wound edge (white lines). (B) Impaired MTOC orientation in cells treated with C3 exoenzyme but not with Y-27632. C6 glioma cells were treated with either C3 exoenzyme or Y-27632 and subjected to the wound-healing assay. After 0 and 8 h, the cells were fixed and the localization of MTOC was identified by staining with antibody to pericentrin. The percentage of cells showing MTOC oriented toward the wound during wound healing is shown ($n = 100$ for each of three independent experiments for each group). (C) Impaired polarization of active Rac in mDia1-depleted cells. Rac activation in control and K2-mediated mDia1 RNAi cells was monitored by FRET with Raichu-Rac for 1 h. Top panels show typical images. Arrows indicate the direction of the wound. Bottom panels show the distribution of Rac activation from the front to tail as examined by FRET ratio ($n = 20$ each). Scale bars, 20 μm.

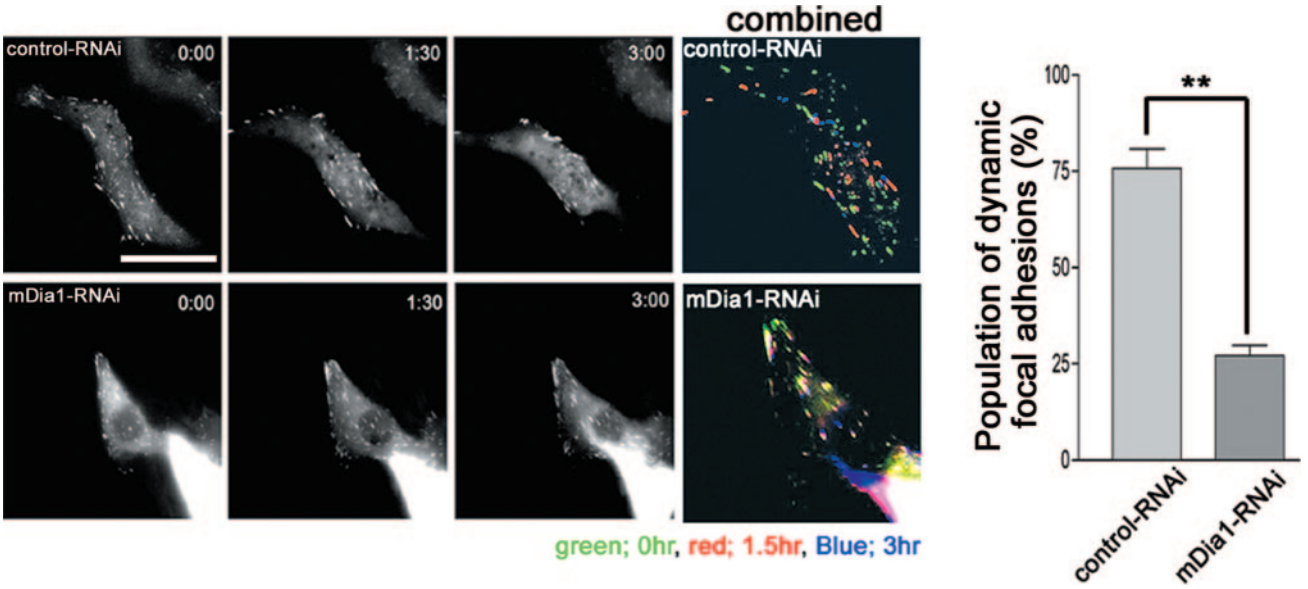

FIG. 3. mDia1 is required for focal adhesion turnover in migrating cells. Typical images of adhesion dynamics as revealed by YFP-paxillin in control and K2-mediated mDia1 RNAi cells are shown, and adhesions at 0, 1.5, and 3 h in each cell are shown in pseudocolor (left). The percentage of adhesions turning over in less than 1 h is shown to the right. **, $P < 0.01$.

Cdc42 between control and mDia1-RNAi cells (data not shown). These results suggest that mDia1 functions to localize active Cdc42 and Apc in the leading edge of migrating cells. To verify this hypothesis, we examined localization of these molecules in cells expressing an active mDia1 mutant, mDia1-ΔN3. Expression of mDia1-ΔN3 induced bipolar elongation of glioma cells in which actin bundles and MTs terminate in the bipolar ends, as we observed previously in HeLa cells (16). Immunofluorescence study revealed accumulation of dot-like Apc signals at each pole of these cells (Fig. 5A). Notably, some of these signals were associated with MTs, and treatment with nocodazole significantly attenuated their accumulation in the periphery (Fig. 5B). Furthermore, FRET analysis for active Cdc42 in the mDia1-ΔN3-expressing cells revealed that the Cdc42 activity is high at both ends with another peak of the activity in the perinuclear region (Fig. 5C).

mDia1 mediates focal adhesion turnover via recruitment of c-Src to and c-Src-mediated p130Cas phosphorylation in adhesions. We then examined how mDia1 induces adhesion turnover. Because adhesion turnover appears to be regulated through Src-mediated Cas phosphorylation and resultant Rac activation (48), we examined Tyr phosphorylation of Cas in mDia1-RNAi cells. In control cells subjected to control RNAi, strong signals for Tyr^{410}-phosphorylated Cas were found in almost all focal adhesions. However, these signals decreased significantly in intensity and size in mDia1-RNAi cells (Fig. 6A). Because Tyr^{410} of p130Cas is targeted by Src kinases, we next examined the localization of active c-Src in control and mDia1 RNAi cells (Fig. 6B, upper and middle panels). Active c-Src, as detected with specific antibody to Tyr^{418}-phosphorylated Src, localized to focal adhesions in control RNAi cells, but this localization was significantly reduced in mDia1 RNAi cells. Conversely, strong signals for phosphorylated Src (Fig. 6B, lower panels) and phosphorylated Cas (data not shown) were found in focal adhesions clustered at the bipolar ends of mDia1-ΔN3-expressing glioma cells. To confirm these findings, we examined the abundance of active c-Src in focal adhesions quantitatively by measuring the ratio of the fluorescence intensity of Tyr^{418}-phosphorylated c-Src and vinculin in each adhesion. This analysis showed that mDia1 RNAi significantly decreased abundance of active c-Src in focal adhesions in migrating cells and that expression of mDia1-ΔN3 significantly increased active c-Src abundance compared to that found in cells transfected with the control vector (Fig. 6B). Accumulation of active c-Src and enhanced Cas phosphorylation in focal adhesions at the poles were more clearly seen in mDia1-ΔN3-expressing HeLa cells (Fig. 7A). Notably, active Src signals were frequently associated with actin bundles targeted to focal adhesions in mDia1-ΔN3-expressing cells, and disruption of actin filaments in these cells with latrunculin B impaired this accumulation (Fig. 7B), indicating that the mDia1-dependent c-Src recruitment is mediated by actin cytoskeleton.

The above findings indicate that mDia1 mediates accumulation of active c-Src in focal adhesions and the resultant Cas phosphorylation. We therefore examined how mDia1 mediates this action. To this end, we used HEK 293 cells and NIH 3T3 cells for better transfection and expression efficiency. It is known that stimulation of NIH 3T3 cells with lysophosphatidic acid (LPA) mimics signaling during directed migration of this line of cells (4). NIH 3T3 cells were susceptible to RNAi with siRNA K2 for mDia1 (data not shown). We first used HEK 293 cells and examined the association between mDia1 and c-Src and the effects of their association on c-Src activation. A previous study reported the SH3-dependent association of Src to the FH1 region of mDia (41). We expressed either wild-type mDia1 or mDia1-ΔN3 together with wild-type c-Src and examined c-Src activation and its association with mDia1 in the presence or absence of PP1, a Src kinase inhibitor (42). As shown in Fig. 8A, expression of mDia1-ΔN3 only slightly enhanced the amount of active c-Src, as assessed by Tyr^{418}-phos-

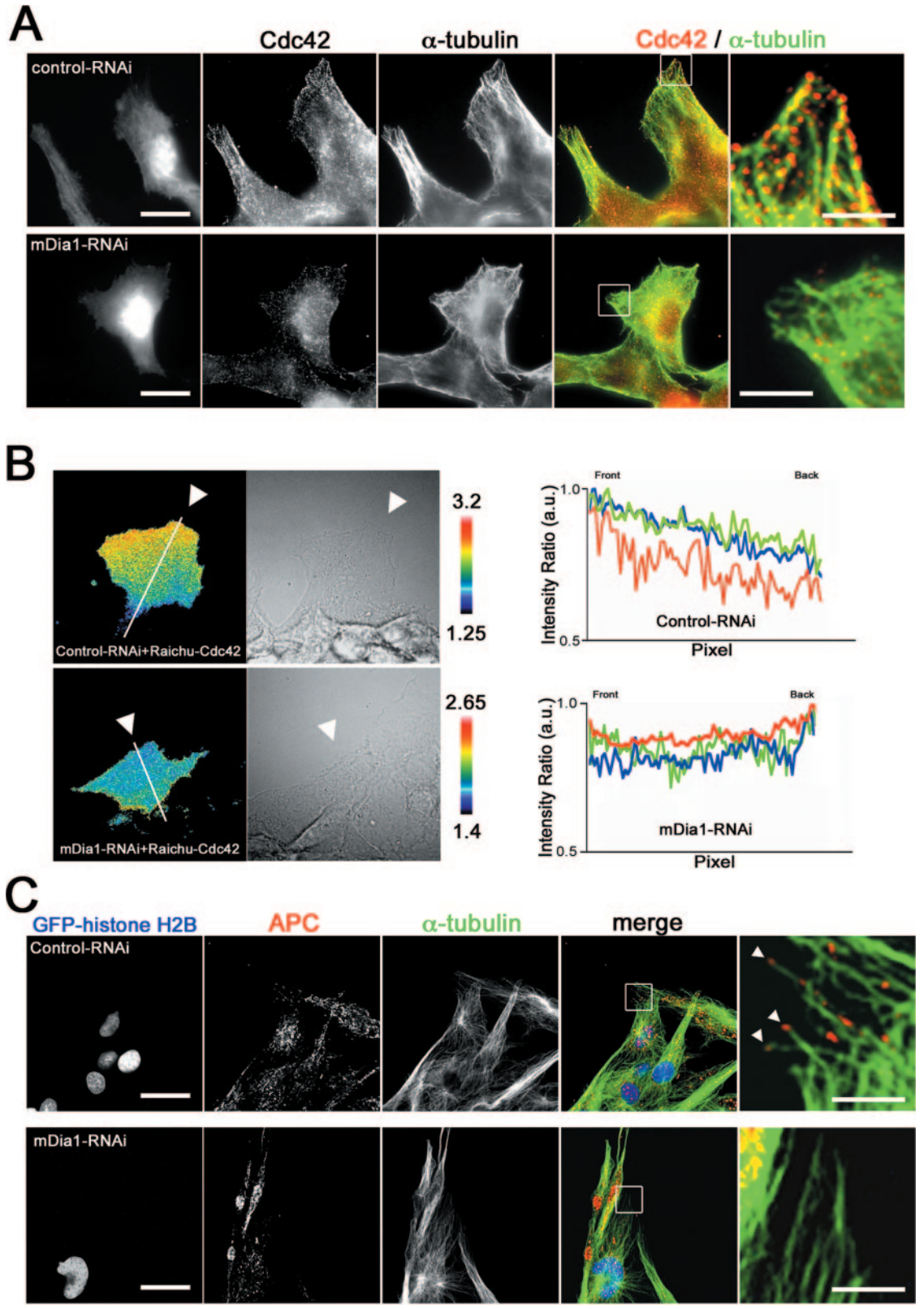

FIG. 4. mDia1 RNAi abolishes accumulation of Cdc42 and Apc in the front of migrating cells. (A) C6 glioma cells were subjected to RNAi and were fixed 8 h after the wounding and stained for Cdc42 (red) and α-tubulin (green). Scale bars, 20 μm. Typical results of three independent experiments, each examining 35 cells, are shown. Right; enlarged images of boxed areas (scale bar, 5 μm). (B) Impaired polarization of active Cdc42 in mDia1-depleted cells. Cdc42 activation in control and K2-mediated mDia1 RNAi was monitored in cells by FRET with Raichu-Cdc42 for 1 h. The Cdc42 activity was measured in three control and three mDia1 RNAi cells along the line in the direction of cell migration from the front to the tail and is shown in arbitrary units (a.u.) with the maximum activity in each cell as 1.0 (right). (C) C6 glioma cells were transfected with siRNA together with pGFP-histone H2B and were fixed 8 h after the wounding with methanol and stained for Apc (red) and α-tubulin (green). A single section of confocal images is shown. Scale bars, 20 μm. Typical results of three independent experiments, each examining 50 cells, are shown. Right; enlarged images of boxed areas (scale bar, 5 μm).

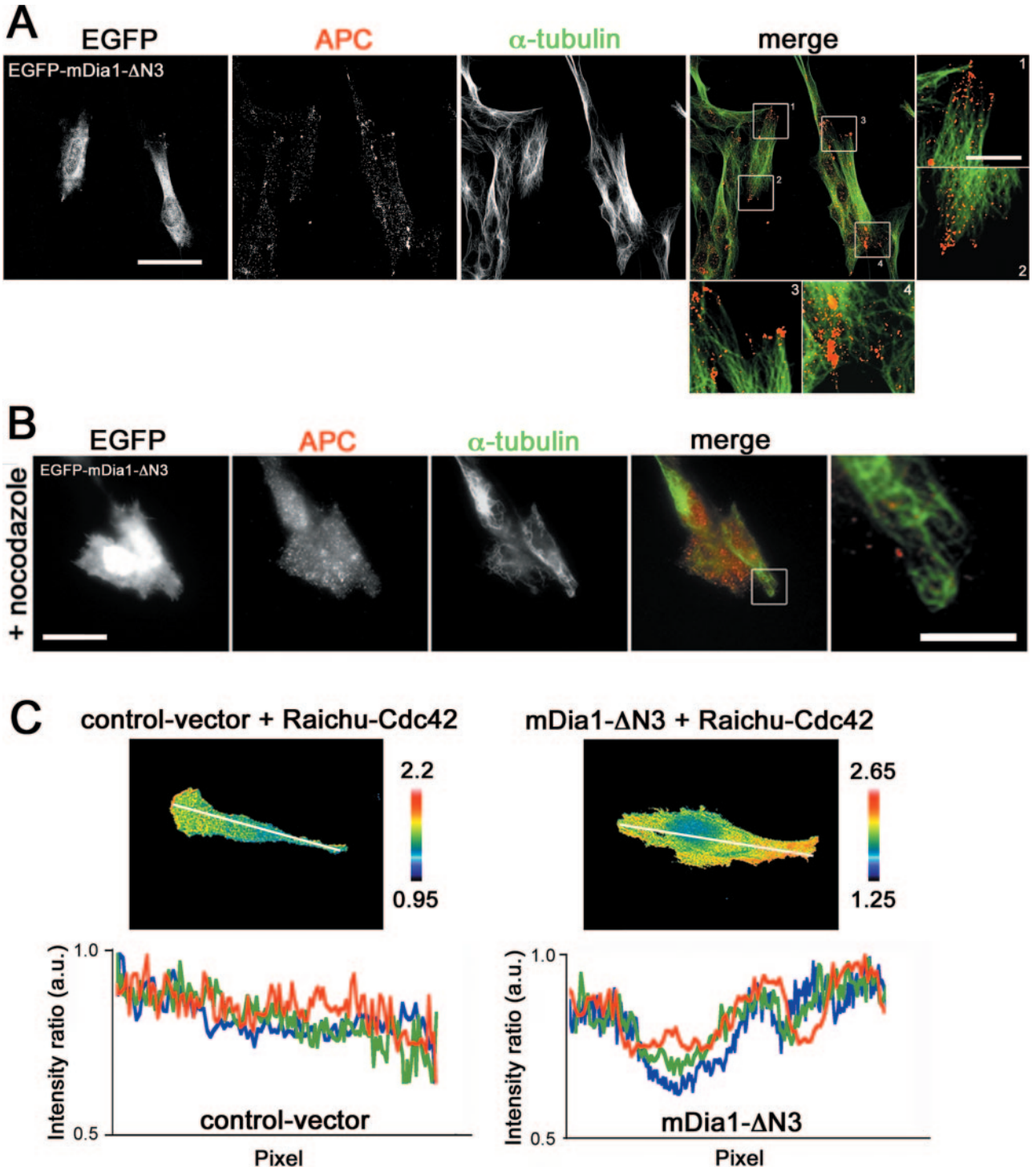

FIG. 5. Active mDia1 enhances accumulation of Cdc42 and Apc in the poles of cells. (A and B) C6 glioma cells transfected with pEGFP-mDia1-ΔN3 were stained for Apc (red) and α-tubulin (green). In panel A, the cells were fixed with methanol and subjected to confocal microscopy. In panel B, the cells were fixed with paraformaldehyde and examined by CCD microscopy. In panel B, the cells were treated with 10 μM nocodazole. Typical cells found in two independent experiments, each examining 20 cells, are shown. Scale bars, 20 μm. The right panels contain enlarged images of the boxed areas in the middle panels (scale bar, 5 μm). (C) C6 glioma cells in sparse culture were transfected with pFL plasmid or pFL-mDia1-ΔN3 together with pRaichu-Cdc42 and subjected to FRET analysis as described for Fig. 4B. The Cdc42 activity was measured along the long axis of three control and three mDia1-ΔN3-expressing cells and is shown in a different color for each cell. a.u., arbitrary units.

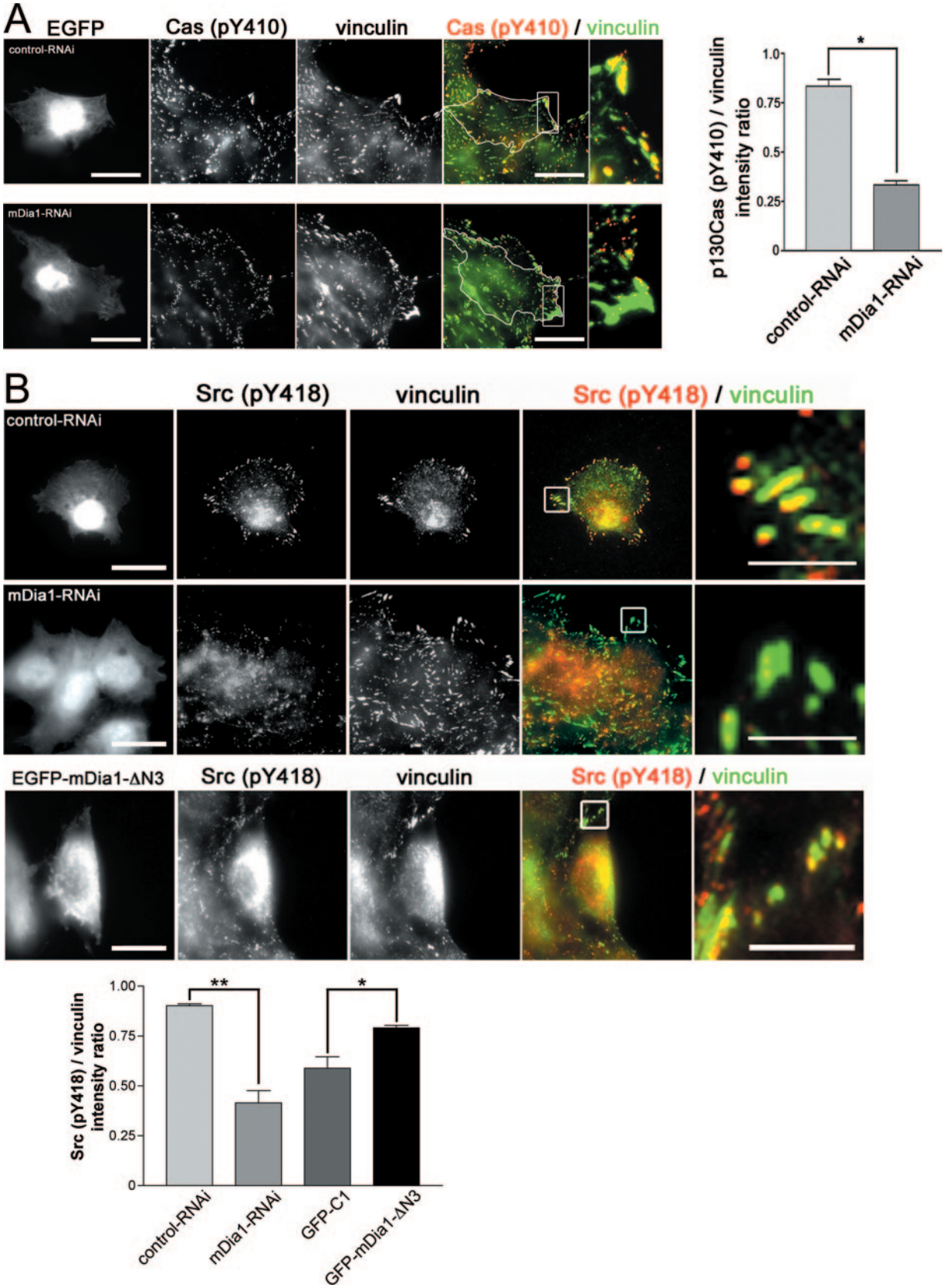

FIG. 6. mDia1 regulates p130Cas phosphorylation and active c-Src recruitment in focal adhesions of migrating cells. (A) mDia1 RNAi reduces Tyr^{410}-phosphorylated Cas in focal adhesions. C6 glioma cells were subjected to control or K2-mediated mDia1 RNAi and were fixed 8 h after the wounding and stained for vinculin (green) and Tyr^{410}-phosphorylated Cas (red). RNAi cells are delineated, and boxed areas are enlarged (right).

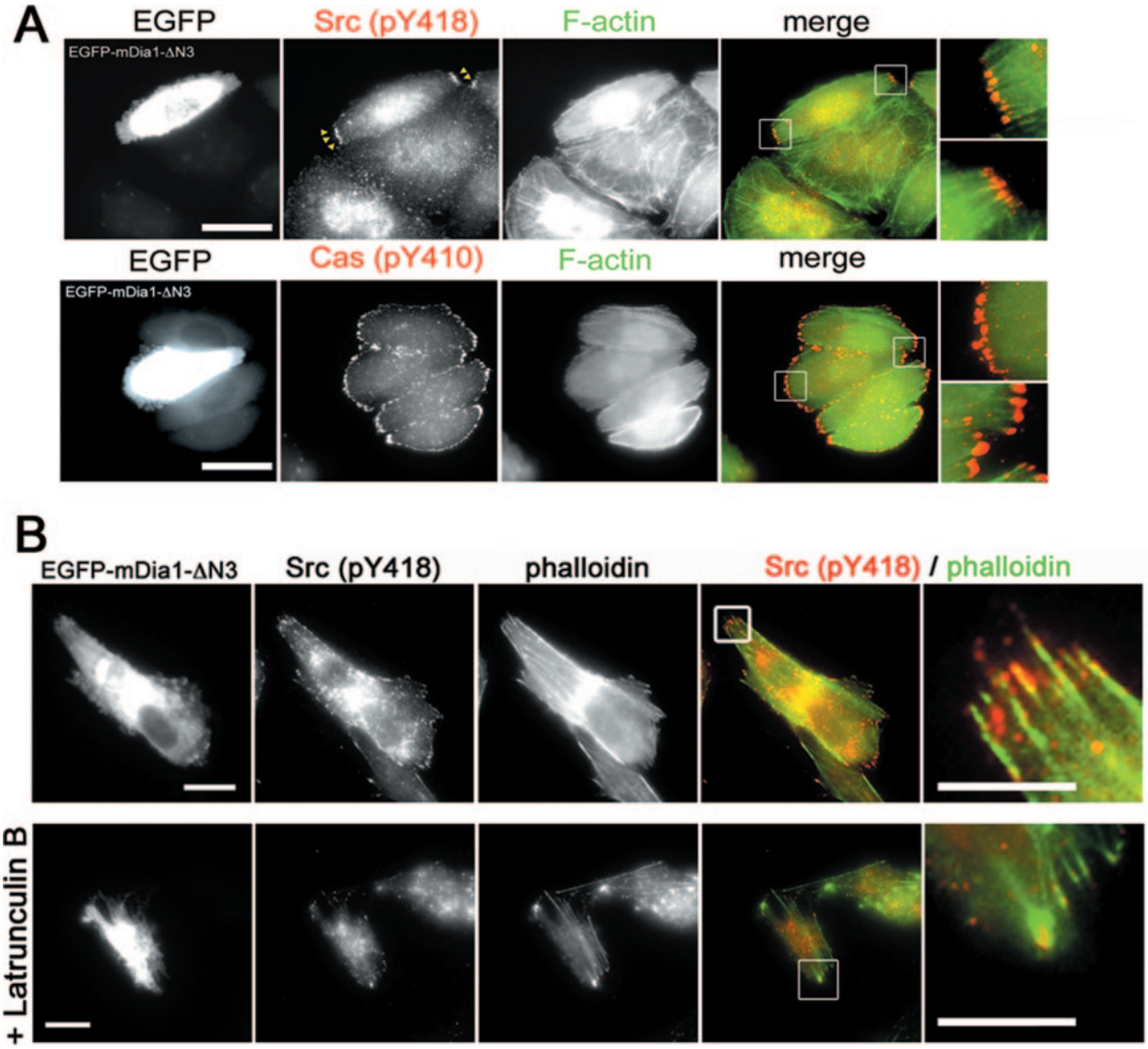

FIG. 7. Accumulation of active c-Src and phosphorylated Cas in focal adhesions and associated actin bundles and impairment of their accumulation by latrunculin. (A) Accumulation of active c-Src and Tyr^{410}-phosphorylated Cas in the poles of HeLa cells expressing mDia1-ΔN3. HeLa cells expressing mDia1-ΔN3 were stained for either Tyr^{418}-phosphorylated c-Src or Tyr^{410}-phosphorylated Cas together with F-actin. Arrowheads indicate adhesions at the poles. Scale bar, 20 μm. (B) C6 glioma cells expressing mDia1-ΔN3 were pretreated with either vehicle (left) or 5 μM latrunculin B (right) for 5 min and stained for Tyr^{418}-phosphorylated c-Src (red) and F-actin (green).

phorylated c-Src, compared to that found in cells expressing wild-type mDia1. On the other hand, mDia1-ΔN3 bound a far greater amount of c-Src than wild-type mDia1. However, this binding was not affected by the addition of PP1, indicating that this binding does not require the enzymatic activity of c-Src. While this result suggested that autophosphorylation at tyrosine 418 was not required for the Src association with mDia1, the c-Src protein that binds to mDia1 is probably in an active

Scale bars, 20 μm. The fluorescence intensity of Tyr^{410}-phosphorylated Cas and vinculin was determined in 10 focal adhesions each of 10 cells by using MetaMorph, and the intensity ratio of Tyr^{410}-phosphorylated Cas to vinculin was calculated (right). *, $P < 0.05$. (B) mDia1 RNAi impairs and expression of active mDia1 augments accumulation of active c-Src in focal adhesions. Control or mDia1-RNAi cells were fixed 8 h after the wounding, or cells in sparse culture were transfected with pEGFP-mDia1-ΔN3 or pEGFP-C1 vector and fixed 12 h after transfection. They were stained for vinculin (green) and Tyr^{418}-phosphorylated c-Src (red). Typical images of cells subjected to control RNAi and mDia1 RNAi and expressing mDia1-ΔN3 are shown in the upper, middle, and lower panels, respectively. Scale bars, 20 μm. Enlarged merged images are shown in the panels to the right (scale bar, 5 μm). The fluorescence intensity of Tyr^{418}-phosphorylated c-Src and vinculin was determined in 10 focal adhesions each of 10 cells subjected to control RNAi, mDia1 RNAi, expression of control vector, or expression of mDia1-ΔN3 by using MetaMorph, and the intensity ratio of Tyr^{418}-phosphorylated c-Src to vinculin was calculated (bottom). * and **, $P < 0.05$ and $P < 0.01$, respectively, for the indicated comparisons.

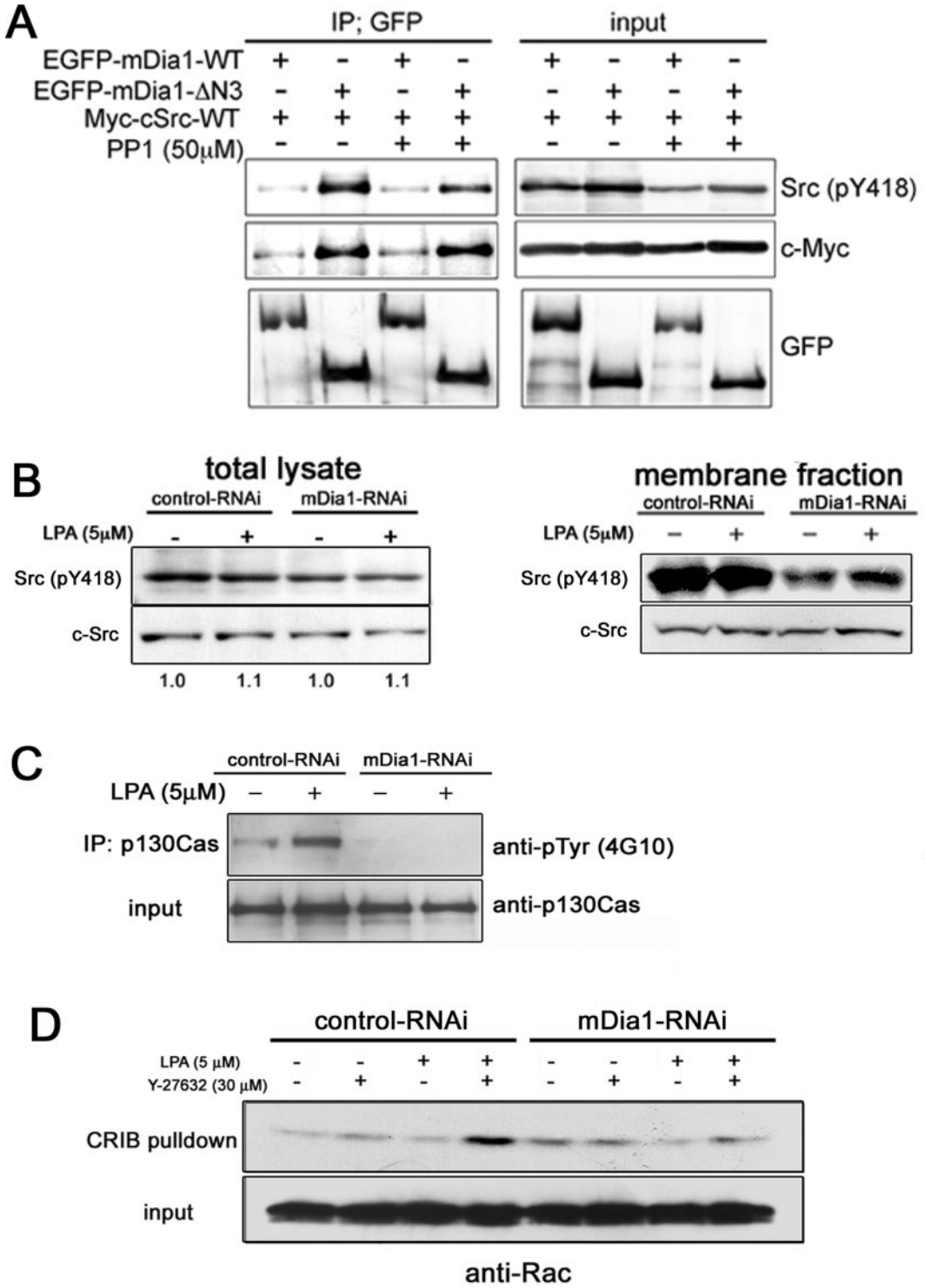

FIG. 8. mDia1 binds to c-Src and mediates its membrane translocation, Cas phosphorylation, and Rac activation. (A) Binding of c-Src by active mDia1. HEK 293 cells expressing GFP fusion of either wild-type (WT) mDia1 or mDia1-ΔN3 and Myc–c-Src were treated with or without 50 μM PP1 for 1 h, lysed, and subjected to immunoprecipitation with anti-GFP antibody. The precipitates and lysates were probed for Tyr^{418}-phosphorylated c-Src, Myc, and GFP. (B) mDia1-dependent translocation of active Src to the membrane. Control or K2-mediated mDia1 RNAi NIH 3T3 cells were stimulated with LPA for 10 min, and their membranes were prepared and subjected with total lysates to immunoblotting for Tyr^{418}-phosphorylated c-Src. Note that the ratio of total c-Src to Tyr^{418}-phosphorylated c-Src did not change with mDia1 depletion. (C) Impaired tyrosine phosphorylation of Cas in mDia1-RNAi cells. NIH 3T3 cells transfected with either control scrambled siRNA or mDia1 siRNA K2 were stimulated with LPA for 10 min, and their lysates were subjected to immunoprecipitation (IP) using anti-p130Cas antibody. The immunoprecipitates were then analyzed by immunoblotting with antibodies to phosphotyrosine and p130Cas. (D) Impaired Rac activation in mDia1-RNAi cells. NIH 3T3 cells subjected to RNAi with control scrambled siRNA or mDia1 siRNA K2 were stimulated with LPA in the presence or absence of Y-27632 and subjected to the pull-down assay for GTP-Rac.

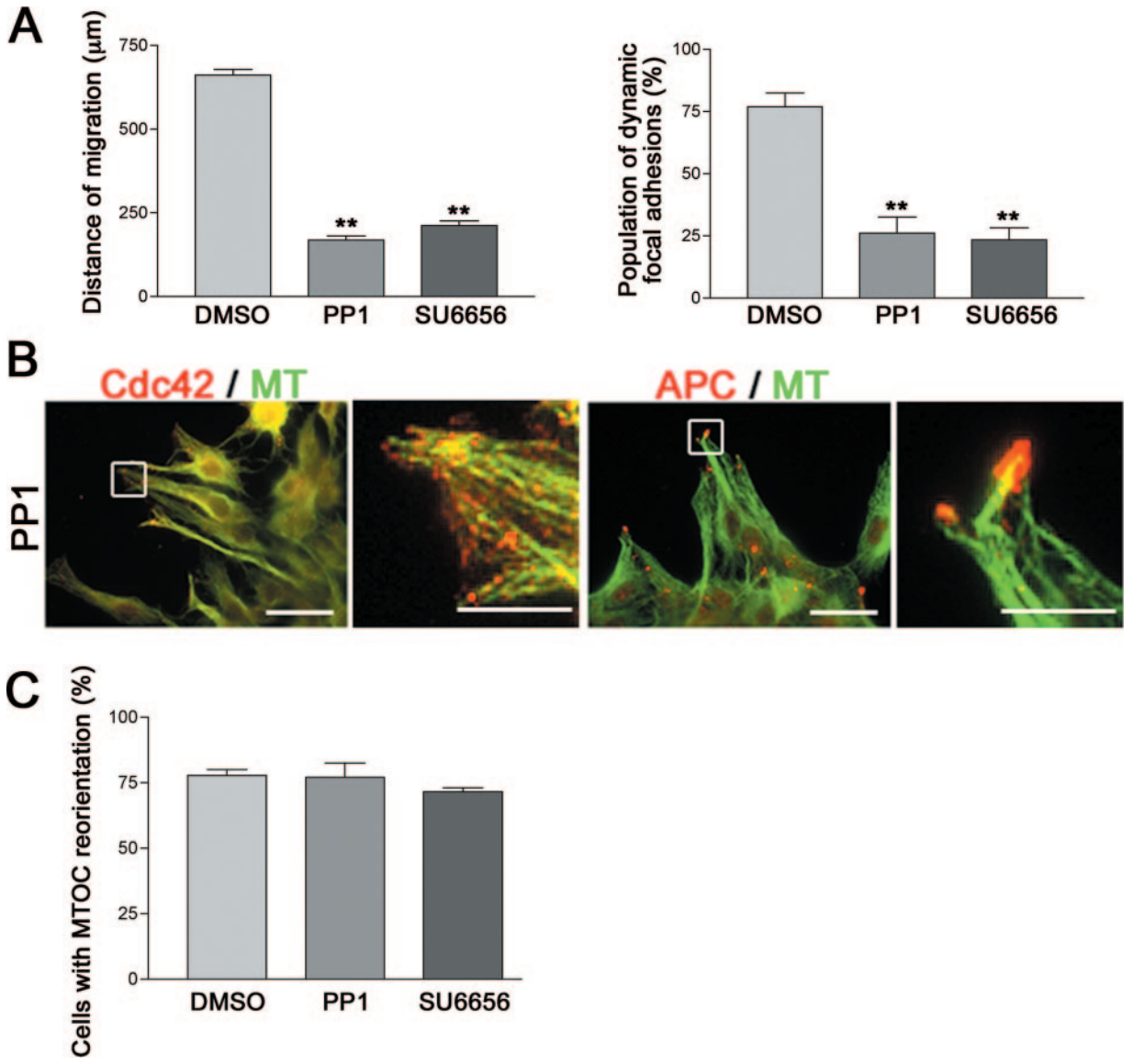

FIG. 9. mDia1 mediates cell polarization in a c-Src-independent manner. C6 glioma cells were treated with vehicle (dimethyl sulfoxide [DMSO]), 30 μM PP1, or 10 μM SU6656; subjected to the wound-healing assay; and examined for motility and adhesion turnover (A), localization of Cdc42 and Apc (B), and MTOC orientation (C). Only cells treated with PP1 are shown in panel B. Scale bars, 20 μm. Enlarged merged images are shown in right (Scale bar, 5 μm). **, $P < 0.01$.

state, because its SH3 region is believed to be available for binding to other protein only in the active state (6). These findings suggest that activation of mDia1 does not influence the overall activation of c-Src in the cell, but facilitates its association with c-Src. This is consistent with findings in NIH 3T3 cells in which we depleted mDia1 by RNAi and examined the level of c-Src activation and the amount of active c-Src translocated to the membrane. As shown in Fig. 8B, mDia1 depletion suppressed the activation of c-Src only slightly and did not affect the amount of membrane-associated total c-Src, but suppressed significantly translocation of Tyr^{418}-phosphorylated active c-Src to the membrane fraction. Translocation of active c-Src to the membrane occurs after its accumulation in adhesions (10), and accumulation of c-Src in adhesions can be assessed by Cas phosphorylation. We therefore quantitatively evaluated the contribution of mDia1 to c-Src accumulation in adhesions by examining Cas phosphorylation in NIH 3T3 cells subjected to control and mDia1 RNAi. Western blot analysis revealed almost complete suppression of tyrosine phosphorylation of Cas in the mDia1 RNAi cells (Fig. 8C). Finally, we examined how much this mDia1–c-Src–Cas pathway is involved in the Rac activation after LPA stimulation. We previously found that LPA stimulation of NIH 3T3 cells activates Rho signaling via a pathway other than ROCK, possibly via mDia1, which potentially leads to Rac activation through Src-dependent Cas phosphorylation and subsequent formation of the Cas-Crk-DOCK180 complex (42). We added Y-27632 in this experiment to enhance mDia1 action by inhibiting ROCK-mediated suppression on the mDia1 pathway (42). In control RNAi cells, the addition of LPA significantly increased the

level of GTP-Rac in the presence of Y-27632. However, no increase in Rac activation was found in mDia1-RNAi cells (Fig. 8D). These results indicate that mDia1 is not primarily involved in c-Src activation but mediates accumulation of active c-Src in adhesions for Rac activation.

mDia1-mediated adhesion turnover and regulation of cell polarization are separate events. Finally, we addressed whether two mDia1-mediated events, regulation of adhesion turnover and that of cell polarization, are interdependent. To examine this issue, we again used PP1. The addition of PP1 interfered with migration and focal adhesion turnover of the glioma cells subjected to the wound-healing assay (Fig. 9A), thus verifying the involvement of c-Src in adhesion turnover in our system. We next examined polarity of the PP1-treated cells that were arrested in their migration at the front edge of the wound. We found that these cells showed normal accumulation of both Cdc42 and Apc at the cell tip (Fig. 9B) and exhibited normally orientated MTOC (Fig. 9C). Essentially the same results were obtained with a different Src inhibitor, SU6656 (Fig. 9).

DISCUSSION

The roles of Rho GTPases in cell migration have been examined by overexpression or microinjection of dominant-active or -negative mutants of each GTPase or by specific inactivation of Rho with botulinum C3 exoenzyme in migrating cells (1, 30). These studies have elucidated the role of Cdc42 in cell polarization and that of Rac in membrane protrusion in the front. However, the role of Rho has been elusive, because inactivation of Rho led to dramatic changes in cell morphology which made further analysis difficult (1, 32). Furthermore, treatment of migrating cells with Y-27632 usually does not affect migration of cells such as rat embryonic fibroblasts (32), negating the role of the Rho-ROCK pathway. Moreover, while the role of mDia1 in cell migration was suggested based on its interaction with c-Src (25, 39), there has been discrepancy in the literature as to its function. For example, Vincente-Manzanares et al. (44) found that expression of an active mDia1 mutant inhibited migration of T cells, which led the authors to suggest that mDia1 regulates cell migration negatively. Quite recently, Goulimari et al. (13) demonstrated that $G\alpha_{12/13}$ localizes Rho and mDia1 in the front edge of migrating cells and this action is essential for LPA-induced directed cell migration. These authors applied RNAi and presented evidence that mDia1 is important for cell migration. Here, we used RNAi for mDia1 and have not only confirmed their findings but further demonstrated that the Rho-mDia1 pathway works for directed cell migration by facilitating both cell polarization and adhesion turnover. Our finding that the Rho-mDia1 pathway regulates MTOC orientation is at odds with the findings by Palazzo et al. (34), who also used C3 exoenzyme but found no effects. This discrepancy may reflect the cell-type-specific difference or may be due to suppression of other Rho GTPases by C3 exoenzyme in our experiment. However, the latter possibility appears unlikely, given that C3 exoenzyme ADP-ribosylates Rac significantly only in the presence of sodium dodecyl sulfate and modifies Cdc42 even less efficiently (7, 18). One possible explanation for the discrepancy is that the findings by Palazzo et al. may be due to insufficient use of C3 exoenzyme that may be indicated by an apparently normal array of MTs in the C3 exoenzyme-treated cells in their study. Insufficient use of C3 exoenzyme can preferentially suppress the ROCK pathway, resulting in dissolution of stress fibers, but keeping the mDia1 pathway intact, because mDia1 responds to a lower level of GTP-Rho than ROCK (2, 41).

By analyzing the mechanism whereby mDia1 regulates focal adhesion turnover, we found that depletion of mDia1 impaired accumulation of active c-Src in focal adhesions and attenuated the resultant Cas phosphorylation. We also found that mDia1 is important in Rac activation through these molecules (this work and reference 42). This is consistent with the previous suggestion by Webb et al. (48) that adhesion turnover is regulated by signaling through Src and focal adhesion proteins such as Cas, Crk, and FAK and the resultant Rac activation and suggests that mDia1 works as a link between Rho and this signaling in focal adhesions. We then analyzed whether mDia1 regulates c-Src activation. We found slight enhancement in the cells overexpressing active mDia1 and slight suppression in the mDia1-depleted cells of c-Src activation. While these changes were reproducibly observed, they were minimal changes compared to a rise in c-Src activation typically observed in cells subjected to stimuli such as bombesin (51). These results suggest that mDia1 does not mediate overall activation of c-Src in the cells. On the other hand, we found that depletion of mDia1 prevented the membrane translocation of active c-Src with a minimal level of suppression on its activation as discussed above. These results strongly argue that the primary action of mDia1 on c-Src is not to activate but to recruit active c-Src to focal adhesions. We further found that in mDia1-ΔN3-expressing cells, active c-Src signals were found on actin bundles targeted to adhesions and its accumulation in adhesions was impaired by the latrunculin treatment. These findings are consistent with the previous findings by Frame and her collaborators (10, 11, 12) that v-Src translocates to the cell periphery through the use of its SH3 domain, via Rho-dependent regulation of the actin cytoskeleton. These researchers recently found that that, upon cell stimulation, c-Src is first transported to RhoB-containing endosomes in the perinuclear region and then transported to focal adhesions (38). However, a Rho effector responsible for this action has remained elusive. Our current findings strongly suggest that mDia1 is a Rho effector responsible for actin-dependent delivery of c-Src to focal adhesions. At present how mDia1 exerts such action remains to be elucidated. We found here that the active form of mDia1 potently bound to c-Src, and we previously showed that active mDia1 moves in the cell in a manner dependent on actin polymerization (14). One possibility therefore is that c-Src forms a complex with mDia1 and this complex moves to focal adhesions by an actin polymerization-driven force. However, it is equally possible that the delivery of c-Src to focal adhesions requires functional mDia1, but that this may be due to the role of mDia1 in actin organization and is not due to direct action. In the yeast *Saccharomyces cerevisiae*, a yeast homolog of mDia1, Bni1p, induces polarized actin cables that are used by an unconventional myosin, myosin V, as tracks to deliver secretory vesicles, organelles, and mRNA (3). These possibilities will be tested in future study. Finally, it should be noted that such actin-dependent mDia1 action on c-Src appears not to be involved in cell polarization, another aspect of mDia1-medi-

ated regulation of cell migration, because treatment of migrating C6 glioma cells with PP1, a Src kinase inhibitor, interfered with adhesion turnover but did not affect cell polarization.

Cdc42 and Apc are critical molecules for cell polarization. Active Cdc42 accumulates both at the Golgi apparatus and in the front of migrating cells, and vesicle-like Cdc42 signals are observed between the two sites (8, 30), indicating delivery of Cdc42 by a vesicular transport system. Apc is delivered along a subset of MTs and accumulates at their plus ends in protruding membranes (26, 31). We have found here that mDia1 depletion affected accumulation of both active Cd42 and Apc in the periphery. These findings suggest that mDia1 facilitates MT-dependent recruitment to or maintenance of active Cdc42 and Apc at the tip of migrating cells. A question is how mDia1 exerts such actions. One possibility is that MTs stabilized by the Rho-mDia1 pathway are responsible for delivery of Cdc42 and/or Apc to the front. If so, there should be a mechanism whereby Cdc42 and/or Apc discriminates between stabilized and unstabilized MTs, because both extend to the front of migrating cells. Alternatively, mDia1 may help Cdc42 and/or Apc be packed in a cargo to be delivered to the front. Or mDia1 might be involved only in activation or transport of active Cdc42, and the Apc accumulation may be a consequence of the peripheral localization of Cdc42, because Etienne-Manneville and Hall (9) reported that active Cdc42 is required for association of Apc with the plus end of MTs. These possibilities will be examined in the future. MTs stabilized by mDia1 may facilitate Rac accumulation in the front, because MT growth activates Rac to promote membrane protrusion (47). These findings suggest that Rho and mDia1 may be activated in the front of migrating cells. Consistently, recent FRET studies have demonstrated that Rho is activated not only in the tail but also in the front of migrating cells, and the Rho activation overlaps with that of Cdc42 in the front (21, 35). mDia1 was also found to accumulate in membrane ruffles and spreading membranes (45).

The Rho GTPases, once thought to influence cell morphogenesis through remodeling of the actin cytoskeleton only, are now known to regulate local dynamics of MTs. The mDia family of proteins is a typical Rho effector mediating actions on both actin and MTs. These proteins not only induce actin nucleation and polymerization, but also stabilize and align microtubules in interphase cells. Our findings thus suggest that mDia1, via its actions on actin and MTs, recruits critical signaling molecules, Apc and Cdc42 as well as c-Src, to their respective sites of action for cell polarization and migration.

ACKNOWLEDGMENTS

We thank Y. Ando for antibody to mDia2; Y. Mimori-Kiyosue for discussion; and K. Nonomura, Y. Kitagawa, and T. Arai for assistance.

This work was supported by grants from a Grant-in-Aid for Specially Promoted Research from the Ministry for Education, Culture, Sports, Science and Technology of Japan. J.M. is supported by the JSPS fellowship for foreign researchers.

REFERENCES

1. **Allen, W. E., D. Zicha, A. J. Ridley, and G. E. Jones.** 1998. A role for Cdc42 in macrophage chemotaxis. J. Cell Biol. **141:**1147–1157.
2. **Arakawa, Y., H. Bito, T. Furuyashiki, T. Tsuji, S. Takemoto-Kimura, K. Kimura, K. Nozaki, N. Hashimoto, and S. Narumiya.** 2003. Control of axon elongation via an SDF-1alpha/Rho/mDia pathway in cultured cerebellar granule neurons. J. Cell Biol. **161:**381–391.
3. **Bretscher, A.** 2003. Polarized growth and organelle segregation in yeast: the tracks, motors, and receptors. J. Cell Biol. **160:**811–816.
4. **Cook, T. A., T. Nagasaki, and G. G. Gundersen.** 1998. Rho guanosine triphosphatase mediates the selective stabilization of microtubules induced by lysophosphatidic acid. J. Cell Biol. **141:**175–185.
5. **Cory, G. O., and A. J. Ridley.** 2002. Cell motility: braking WAVEs. Nature **418:**732–733.
6. **Cowan-Jacob, S. W., G. Fendrich, P. W. Manley, W. Jahnke, D. Fabbro, J. Liebetanz, and T. Meyer.** 2005. The crystal structure of a c-Src complex in an active conformation suggests possible steps in c-Src activation. Structure **13:**861–871.
7. **Dillon, S. T., and L. A. Feig.** 1995. Purification and assay of recombinant C3 transferase. Methods Enzymol. **256:**174–184.
8. **Etienne-Manneville, S., and A. Hall.** 2001. Integrin-mediated activation of Cdc42 controls cell polarity in migrating astrocytes through PKCzeta. Cell **24:**489–498.
9. **Etienne-Manneville, S., and A. Hall.** 2003. Cdc42 regulates GSK-3 and adenomatous polyposis coli to control cell polarity. Nature **421:**753–756.
10. **Fincham, V. J., and M. C. Frame.** 1998. The catalytic activity of Src is dispensable for translocation to focal adhesions but controls the turnover of these structures during cell motility. EMBO J. **17:**81–92.
11. **Fincham, V. J., V. G. Brunton, and M. C. Frame.** 2000. The SH3 domain directs acto-myosin-dependent targeting of v-Src to focal adhesions via phosphatidylinositol 3-kinase. Mol. Cell. Biol. **20:**6518–6536.
12. **Fincham, V. J., M. Unlu, V. G. Brunton, J. D. Pitts, J. A. Wyke, and M. C. Frame.** 1996. Translocation of Src kinase to the cell periphery is mediated by the actin cytoskeleton under the control of the Rho family of small G proteins. J. Cell Biol. **135:**1551–1564.
13. **Goulimari, P., T. M. Kitzing, H. Knieling, D. T. Brandt, S. Offermanns, and R. Grosse.** 2005. $G\alpha_{12/13}$ is essential for directed cell migration and localized Rho-Dia1 function. J. Biol. Chem. **51:**42242–42251.
14. **Higashida, C., T. Miyoshi, A. Fujita, F. Oceguera-Yanez, J. Monypenny, Y. Andou, S. Narumiya, and N. Watanabe.** 2004. Actin polymerization-driven molecular movement of mDia1 in living cells. Science **303:**2007–2010.
15. **Hirose, M., T. Ishizaki, M. Uehata, O. Kranenburg, W. H. Moolenaar, F. Matsumura, M. Maekawa, H. Bito, and S. Narumiya.** 1998. Molecular dissection of the Rho-associated protein kinase (p160ROCK)-regulated neurite remodeling in neuroblastoma N1E-115 cells. J. Cell Biol. **141:**1625–1636.
16. **Ishizaki, T., Y. Morishima, M. Okamoto, T. Furuyashiki, T. Kato, and S. Narumiya.** 2001. Coordination of microtubules and the actin cytoskeleton by the Rho effector mDia1. Nat. Cell Biol. **3:**8–14.
17. **Itoh, R. E., K. Kurokawa, Y. Ohba, H. Yoshizaki, N. Mochizuki, and M. Matsuda.** 2002. Activation of Rac and Cdc42 video imaged by fluorescent resonance energy transfer-based single-molecule probes in the membrane of living cells. Mol. Cell. Biol. **22:**6582–6591.
18. **Just, I., C. Mohr, G. Schallehn, L. Menard, J. R. Didsbury, J. Vandekerckhove, J. van Damme, and K. Aktories.** 1992. Purification and characterization of an ADP-ribosyltransferase produced by Clostridium limosum. J. Biol. Chem. **267:**10274–10280.
19. **Kimura, K., M. Ito, M. Amano, K. Chihara, Y. Fukata, M. Nakafuku, B. Yamamori, J. Feng, T. Nakano, K. Okawa, A. Iwamatsu, and K. Kaibuchi.** 1996. Regulation of myosin phosphatase by Rho and Rho-associated kinase (Rho-kinase). Science **273:**245–248.
20. **Kraynov, V. S., C. Chamberlain, G. M. Bokoch, M. A. Schwartz, S. Slabaugh, and K. M. Hahn.** 2000. Localized Rac activation dynamics visualized in living cells. Science **290:**333–337.
21. **Kurokawa, K., and M. Matsuda.** 2005. Localized RhoA activation as a requirement for the induction of membrane ruffling. Mol. Biol. Cell **16:**4294–4303.
22. **Laukaitis, C. M., D. J. Webb, K. Donais, and A. F. Horwitz.** 2001. Differential dynamics of alpha 5 integrin, paxillin, and alpha-actinin during formation and disassembly of adhesions in migrating cells. J. Cell Biol. **153:**1427–1440.
23. **Li, F., and H. N. Higgs.** 2003. The mouse Formin mDia1 is a potent actin nucleation factor regulated by autoinhibition. Curr. Biol. **13:**1335–1340.
24. **Maekawa, M., T. Ishizaki, S. Boku, N. Watanabe, A. Fujita, A. Iwamatsu, T. Obinata, K. Ohashi, K. Mizuno, and S. Narumiya.** 1999. Signaling from Rho to the actin cytoskeleton through protein kinases ROCK and LIM-kinase. Science **285:**895–898.
25. **Meng, W., M. Numazaki, K. Takeuchi, Y. Uchibori, Y. Ando-Akatsuka, M. Tominaga, and T. Tominaga.** 2004. DIP (mDia interacting protein) is a key molecule regulating Rho and Rac in a Src-dependent manner. EMBO J. **23:**760–771.
26. **Mimori-Kiyosue, Y., N. Shiina, and S. Tsukita.** 2000. Adenomatous polyposis coli (APC) protein moves along microtubules and concentrates at their growing ends in epithelial cells. J. Cell Biol. **148:**505–518.
27. **Mochizuki, N., S. Yamashita, K. Kurokawa, Y. Ohba, T. Nagai, A. Miyawaki, and M. Matsuda.** 2001. Spatio-temporal images of growth-factor-induced activation of Ras and Rap1. Nature **411:**1065–1068.
28. **Morii, N., and S. Narumiya.** 1995. Preparation of native and recombinant Clostridium botulinum C3 ADP-ribosyltransferase and identification of Rho proteins by ADP-ribosylation. Methods Enzymol. **256:**196–206.

29. **Nakamoto, T., R. Sakai, H. Honda, S. Ogawa, H. Ueno, T. Suzuki, S.-I. Aizawa, Y. Yazaki, and H. Hirai.** 1997. Requirements for localization of p130^{cas} to focal adhesions. Mol. Cell. Biol. **17:**3884–3897.
30. **Nalbant, P., L. Hodgson, V. Kraynov, A. Touychkine, and K. M. Hahn.** 2004. Activation of endogenous Cdc42 visualized in living cells. Science **305:**1615–1619.
31. **Nathke, I. S., C. L. Adams, P. Polakis, J. H. Sellin, and W. J. Nelson.** 1996. The adenomatous polyposis coli tumor suppressor protein localizes to plasma membrane sites involved in active cell migration. J. Cell Biol. **134:**165–179.
32. **Nobes, C. D., and A. Hall.** 1999. Rho GTPases control polarity, protrusion, and adhesion during cell movement. J. Cell Biol. **144:**1235–1244.
33. **Oceguera-Yanez, F., K. Kimura, S. Yasuda, C. Higashida, T. Kitamura, Y. Hiraoka, T. Haraguchi, and S. Narumiya.** 2005. Ect2 and MgcRacGAP regulate the activation and function of Cdc42 in mitosis. J. Cell Biol. **168:**221–232.
34. **Palazzo, A. F., H. L. Joseph, Y. J. Chen, D. L. Dujardin, A. S. Alberts, K. K. Pfister, R. B. Vallee, and G. G. Gundersen.** 2001. Cdc42, dynein, and dynactin regulate MTOC reorientation independent of Rho-regulated microtubule stabilization. Curr. Biol. **11:**1536–1541.
35. **Pertz, O., L. Hodgson, R. L. Klemke, and K. M. Hahn.** 2006. Spatiotemporal dynamics of RhoA activity in migrating cells. Nature **440:**1069–1072.
36. **Ridley, A. J., M. A. Schwartz, K. Burridge, R. A. Firtel, M. H. Ginsberg, G. Borisy, J.T. Parsons, and A. R. Horwitz.** 2003. Cell migration: integrating signals from front to back. Science **302:**1704–1709.
37. **Rodriguez, O. C., A. W. Schaefer, C. A. Mandato, P. Forscher, W. M. Bement, and C. M. Waterman-Storer.** 2003. Conserved microtubule-actin interactions in cell movement and morphogenesis. Nat. Cell Biol. **5:**599–609.
38. **Sandilands, E., C. Cans, V. J. Fincham, V. G. Brunton, H. Mellor, G. C. Prendergast, J. C. Norman, G. Superti-Furga, and M. C. Frame.** 2004. RhoB and actin polymerization coordinate Src activation with endosome-mediated delivery to the membrane. Dev. Cell **7:**855–869.
39. **Satoh, S., and T. Tominaga.** 2001. mDia-interacting protein acts downstream of Rho-mDia and modifies Src activation and stress fiber formation. J. Biol. Chem. **276:**39290–39294.
40. **Sekine, A., M. Fujiwara, and S. Narumiya.** 1989. Asparagine residue in the rho gene product is the modification site for botulinum ADP-ribosyltransferase. J. Biol. Chem. **264:**8602–8605.
41. **Tominaga, T., E. Sahai, P. Chardin, F. McCormick, S. A. Courtneidge, and A. S. Alberts.** 2000. Diaphanous-related formins bridge Rho GTPase and Src tyrosine kinase signaling. Mol. Cell **5:**13–25.
42. **Tsuji, T., T. Ishizaki, M. Okamoto, C. Higashida, K. Kimura, T. Furuyashiki, Y. Arakawa, R. B. Birge, T. Nakamoto, H. Hirai, and S. Narumiya.** 2002. ROCK and mDia1 antagonize in Rho-dependent Rac activation in Swiss 3T3 fibroblasts. J. Cell Biol. **157:**819–830.
43. **Uehata, M., T. Ishizaki, H. Satoh, T. Ono, T. Kawahara, T. Morishita, H. Tamakawa, K. Yamagami, J. Inui, M. Maekawa, and S. Narumiya.** 1997. Calcium sensitization of smooth muscle mediated by a Rho-associated protein kinase in hypertension. Nature **389:**990–994.
44. **Vicente-Manzanares, M., M. Rey, M. Perez-Martinez, M. Yanez-Mo, D. Sancho, J. R. Cabrero, O. Barreiro, H. de la Fuente, K. Itoh, and F. Sanchez-Madrid.** 2003. The RhoA effector mDia is induced during T cell activation and regulates actin polymerization and cell migration in T lymphocytes. J. Immunol. **171:**1023–1034.
45. **Watanabe, N., P. Madaule, T. Reid, T. Ishizaki, G. Watanabe, A. Kakizuka, Y. Saito, L. Nakao, B. M. Jockusch, and S. Narumiya.** 1997. p140mDia, a mammalian homolog of Drosophila diaphanous, is a target protein for Rho small GTPase and is a ligand for profilin. EMBO J. **16:**3044–3056.
46. **Watanabe, N., T. Kato, A. Fujita, T. Ishizaki, and S. Narumiya.** 1999. Cooperation between mDia1 and ROCK in Rho-induced actin reorganization. Nat. Cell Biol. **1:**136–143.
47. **Waterman-Storer, C. M., R. A. Worthylake, B. P. Liu, K. Burridge, and E. D. Salmon.** 1999. Microtubule growth activates Rac1 to promote lamellipodial protrusion in fibroblasts. Nat. Cell Biol. **1:**45–50.
48. **Webb, D. J., K. Donais, L. A. Whitmore, S. M. Thomas, C. E. Turner, J. T. Parsons, and A. F. Horwitz.** 2004. FAK-Src signalling through paxillin, ERK and MLCK regulates adhesion disassembly. Nat. Cell Biol. **6:**154–161.
49. **Wen, Y., C. H. Eng, J. Schmoranzer, N. Cabrera-Poch, E. J. Morris, M. Chen, B. J. Wallar, A. S. Alberts, and G. G. Gundersen.** 2004. EB1 and APC bind to mDia to stabilize microtubules downstream of Rho and promote cell migration. Nat. Cell Biol. **6:**820–830.
50. **Worthylake, R. A., S. Lemoine, J. M. Watson, and K. Burridge.** 2001. RhoA is required for monocyte tail retraction during transendothelial migration. J. Cell Biol. **154:**147–160.
51. **Wu, S. S., K. Yamauchi, and E. Rozengurt.** 2005. Bombesin and angiotensin 2 rapidly stimulate Src phosphorylation at Tyr-418 fibroblasts and intestinal epithelial cells through a PP2-insensitive pathway. Cell. Signal. **17:**93–102.
52. **Zaidel-Bar, R., C. Ballestrem, Z. Kam, and B. Geiger.** 2003. Early molecular events in the assembly of matrix adhesions at the leading edge of migrating cells. J. Cell Sci. **116:**4605–4613.
53. **Zicha, D., G. A. Dunn, and A. F. Brown.** 1991. A new direct-viewing chemotaxis chamber. J. Cell Sci. **99:**769–775.